



Characteristics of silver-doped carbon nanotube coating destined for medical applications

Dorota Rogala-Wielgus^{*}, Beata Majkowska-Marzec, Andrzej Zieliński

Division of Biomaterials Technology, Institute of Manufacturing and Materials Technology, Faculty of Mechanical Engineering and Ship Technology, Gdańsk University of Technology, 11 Narutowicza str., 80-233 Gdańsk, Poland

ARTICLE INFO

Keywords:

Carbon nanotubes
Silver
Composite coatings
Young's modulus
Adhesion
Corrosion resistance

ABSTRACT

Carbon nanotubes are materials demonstrating outstanding mechanical, chemical, and physical properties and are considered coatings of titanium implants. The present research is aimed to characterize the microstructure and properties of the multi-wall carbon nanotubes (MWCNTs) layer decorated with silver nanoparticles (Ag NPs) on the Ti13Nb13Zr alloy destined for long-term implants. The electrophoretic deposition of coatings was performed in a two-stage process, at first at 0.25 wt. pct. of MWCNTs, and next at 0.30 wt. pct. of Ag NPs content in the bath. The SEM, EDS, AFM, Raman spectroscopy, nanoindentation tests, nano-scratch test, wettability assessments, and corrosion tests were carried out. The effects of the presence of Ag NPs onto the MWCNTs coating were observed as the roughness increased to 0.380 μm and thickness to 5.26 μm , the improved adhesion and corrosion resistance, the water contact angle of 62.94°, the decreased nano-hardness, Young's modulus and resistance to plastic deformation under load, and slightly improved adhesion. The obtained results can be explained by a specific two-layer structure of the coating, in which the Ag NPs agglomerates create the coating less porous and permeable, but softer structure. Future research will focus on the improvement of the adhesion of the component coatings in different ways.

1. Introduction

Titanium and its alloys have excellent biocompatibility, the appropriate mechanical properties except for hardness, and are highly resistant to corrosion, while demonstrating low bioactivity and no bactericidal protection. Therefore, they are usually surface-modified by several well-known techniques [1–4], mainly to attain antibacterial properties [5–8] and bioactivity [9–11].

Nanotechnologies play an important role in civilization's progress. The different nanoforms, especially nanoparticles, nanofilms, and surface nanostructuring are increasingly applied in the economy. The nanoparticles and nanofilms are nowadays proposed for different medical and pharmaceutical applications [12–15], in electronics and energy storage [16–18], environment protection [19,20], agriculture and food packaging [21,22], for inkjets [23], and in other applications. Among them, appear such nanoforms as carbon nanotubes (CNTs) and silver nanoparticles (Ag NPs), the components of coatings developed in the present research.

Carbon nanotubes and related structures include single-walled carbon nanotubes (SWCNTs), multi-wall carbon nanotubes (MWCNTs),

nanohorns, nanobus, and nanotorus known for their outstanding mechanical, electronic, thermal, optical, and chemical properties [24,25]. Specifically, they approach 30 GPa in tensile strength, can have an elastic modulus of about 1 GPa [26,27], and demonstrate high mechanical stiffness, remarkable thermal conductivity, and electrical semiconductivity or superconductivity [25,28]. The CNTs were considered, among others, for use in diagnostic and therapy [28–30], specifically in drug transport [28], as gene carriers [31], in bone tissue regeneration [32], neuroscience [29,33], and to improve the wear resistance of Ti implants [34].

The coatings based on CNTs are less popular than composite materials because of their specific loose microstructure. They were developed to enhance the adsorption of proteins on titanium [35], improving the resistance to tribocorrosion in biological conditions [36], strengthening hydroxyapatite (HAp) deposits [37–40], as HAp-collagen [41], HAp-Ti [42], and CNTs with Cu NPs or titania [43,44], with collagen-acrylic acid [45], polysiloxane [46], or Al₃Ti-Cu-SiC [47], and also as electrospun chitosan/CNT coatings on Mg alloy [48].

The silver nanoparticles Ag NPs are well-known for their strong antibacterial properties [49]. In medicine, the chitosan – Ag NPs [50],

^{*} Corresponding author.

E-mail address: dorota.wielgus@pg.edu.pl (D. Rogala-Wielgus).

silk fibroin/Ag co-functionalized strontium titanate nanotubes [51], Ag NPs – polyaniline [52], Ag NPs – hydroxychloroquine [53], hyaluronic acid – Ag NPs [54], PEG – Ag NPs [55], nanosilver - chitosan/Eudragit polymers [56–58]. In particular, they were proposed for the improvement of behavior of orthodontic brackets [59], for drug delivery [60] and bone engineering [61,62], as plant-based Ag NPs for cardioprotective treatment [63], in cancer therapy [64–66], anti-diabetic treatment [67], wound healing [68], and for kidney injuries [69]. The other popular technical applications include anti-corrosion protection [70–74], environment protection [75,76], conductive inks [77], covering the touch screen panels [78], in antibacterial protection of cultural monuments [79], to improve thermal properties [80] and reduce the wear of silicon-based components [81], and in photocatalysis [82]. The antibacterial barrier on titanium can also be achieved by other approaches, as recently proposed strontium titanate nanotubes functionalized with peptides [83,84], and Mg-Cu/doped titanium oxide layer [85].

Carbon nanotubes together with Ag nanoparticles are also frequent. Silver nanoparticles are often used as antibacterial compounds in bulk composites or coatings. They are considered for catalysis in enhancing oxygen reduction [86], and in electrochemistry as the CNTs-silver borate for ion-selective electrodes [87]. They can be used in construction materials such as a reinforcement of the copper matrix composites [88], CNTs, Ag NPs, and PVA for electrospun nanofiber mate [89], as titanium dioxide functionalized MWCNTs with Ag NPs to reinforce PU nanofibers [90], and PTFE, Ag NPs, CNTs, and graphene oxide (GO) for cement pastes [91]. Similar solutions are considered in electronics and energy storage as the combination of PP, CNTs, and Ag for electromagnetic interference shielding [92], for hydrogen storage [93], as film composed of Ag selenide and MWCNTs to improve surface thermo-electric properties [94], to increase durability of silicon solar cells [95], as Ag-decorated MnO₂/CNTs electrodes for supercapacitors [96], together with GO for doping of amorphous selenium for optoelectronic devices [97,98].

Our previous research was focused on checking the mechanical properties of the coating composed of MWCNTs, hydroxyapatite, Ag NPs, and Cu NPs [18] demonstrating satisfactory values for Young's modulus of 8.88 GPa, but improper hardness, wettability, and adhesion. The present research aims to verify whether the MWCNTs layer decorated with Ag nanoparticles at a three-fold higher amount of silver, desired for antibacterial prevention, has all necessary mechanical, corrosion, and wettability properties, and how microstructural features can explain them.

2. Materials and methods

2.1. Materials

The 20 mm in diameter and 4 mm thick samples of Ti13Nb13Zr alloy (MR) (Xi'an SATE Metal Materials Development Co., China), composed of 13.18 wt. pct. Nb, 13.49 wt. pct. Zr, 0.085 wt. pct. Fe, 0.035 wt. pct. C, 0.004 wt. pct. H, 0.078 wt. pct. O, < 0.001 wt. pct. S, 0.055 wt. pct. Hf and remaining Ti were cut from the rod and grounded with abrasive paper ended at # 800 grit (Saphir 330, ATM GmbH, Germany). The surfaces were subsequently rinsed with acetone (Chempur, Poland) for 2 min and distilled water, air-dried, pickled in 5% HF (Chempur, Poland) for 30 s, and again water-rinsed.

2.2. Electrophoretic deposition

The MWCNTs modified with –COOH (3D-Nano, Poland), of outer diameter 10–15 nm, inner diameter 2–6 nm, length 1–10 μm, number of walls 3–15, were deposited on Ti13Nb13Zr substrate using EPD method at the parameters shown in Table 1 and based on previous research [43]. The MWCNTs were ultrasonically dispersed in distilled water by stirring for 1 h. The DC power source (MCP/SPN110–01 C, Shanghai MCP Corp.,

Table 1

The parameters of the EPD synthesis of MWCNTs coatings.

Coating assignment	Deposited material	Component content (wt. pct.)	Deposition time (min)	Deposition voltage (V)
MWCNTs	MWCNTs	0.25	1	20
MWCNTs/Ag	MWCNTs	0.25	1	20
	Ag NPs	0.30	4	50

The Ag layer was prepared by EPD on the previous MWCNTs layer in the bath containing 0.30 wt. pct. of Ag NPs (Hongwu International Group Ltd., China) of 30 nm size as an average, and 1 wt. pct. of Polysorbate 20 (Tween 20, Sigma-Aldrich, Poland) in isopropanol, ultrasonically dispersed for 2 h.

China), and two electrodes, an anode of the Ti13Zr13Nb alloy and a counter electrode of the stainless steel 316 L were placed parallel to each other at a distance of 5 mm.

2.3. Investigations of the microstructural features

A high-resolution scanning electron microscope (SEM JEOL JSM-7800 F, Japan) with a LED detector, was applied at a 5 kV to examine the morphology of surfaces and cross-sections of coatings. The surface topography was evaluated using an atomic force microscope (AFM NaniteAFM, Nanosurf, Great Britain) in the non-contact mode at 20 mN force. The average roughness index S_a was estimated based on 512 lines made in the area of $80.4 \times 80.4 \mu\text{m}^2$. The cross-sections were prepared using a pressure-sensitive tape test according to the ASTM D3359–97 to assess the thickness of the coatings. The chemical composition of the coatings was investigated by the X-ray energy dispersive spectrometer (EDS) (Octane Elite 25, EDAX Ametek, USA).

2.4. Wettability assessment

The wettability was examined at room temperature by the water contact angle (CA) measurements (Contact Angle Goniometer, Zeiss, Germany). The falling drop method was applied at 5 s time for a dropout. Each specimen was tested three times in different areas, and the means and standard deviations (SD) were calculated.

2.5. Raman spectroscopy

The Raman microscope (Renishaw InVia plc., UK) with an EMCCD detector (Andor Technology Ltd, Oxford Instruments, Belfast, UK) and the objective lens set at 20x was used. The results were the graphs of the means and SDs based on 100 points. The wavelength of the laser during tests was 532 nm, the single measurement time 1 s or 0.5 s, the measurement counts 5 or 10, and the laser power 0.2 or 1 mW, for the coatings without or with Ag NPs, respectively.

2.6. Nanoindentation testing

The NanoTest™ Vantage (Micro Materials, Great Britain) with a Berkovich indenter was used. The 25 measurements were carried out on each sample, at the maximum applied force of 10 mN, loading and unloading times set up at 20 s, the dwell period at a maximum load of 10 s, and the distance between the subsequent indents of 20 μm. The Oliver and Pharr method was used to determine the load–displacement (L–D) curve, and then the surface nanohardness (H), reduced Young's modulus (E_r), maximum indent depth (h_{max}), plasticity energy (PE), and elastic recovery energy (ERE) with an integrated software. To assess the surface Young's modulus (E), the Poisson's ratio (ν) values of 0.25, 0.37, and 0.36, for the MWCNTs coating, Ag NPs, and Ti13Nb13Zr alloy [40,99]. Then the Halpin-Tsai (H-P) model was used to evaluate the ν , E, and H values for unidirectional composite MWCNTs/Ag coating, as described in [44]. The volume fraction [100] was calculated assuming the density of 4.0 g cm^{-3} [99] and 2.1 g cm^{-3} [101] for the MWCNTs and Ag NPs

[99,101], respectively. Therefore, the assessed ν value for the MWCNTs/Ag coating was set at 0.213.

Nanoscratch tests were performed also with NanoTest™ Vantage. During the scratch tests, the load increased from 0 to 200 mN, and the loading rate and distance were 1.3 mN s^{-1} , and $500 \mu\text{m}$, respectively. The assessment of coating adhesion was based on an abrupt change in frictional force (F_f) and indicated as critical load (L_c). In the end, the scratches were observed under an optical microscope (BX51, OLYMPUS,

Japan).

2.7. Corrosion tests

The potentiodynamic polarization tests were carried out with a potentiostat (Atlas 0531, Atlas Sollich, Poland), with software calculating the corrosion potential (E_{corr}), and corrosion current density (j_{corr}) based on Tafel extrapolation. The sample was the working electrode,

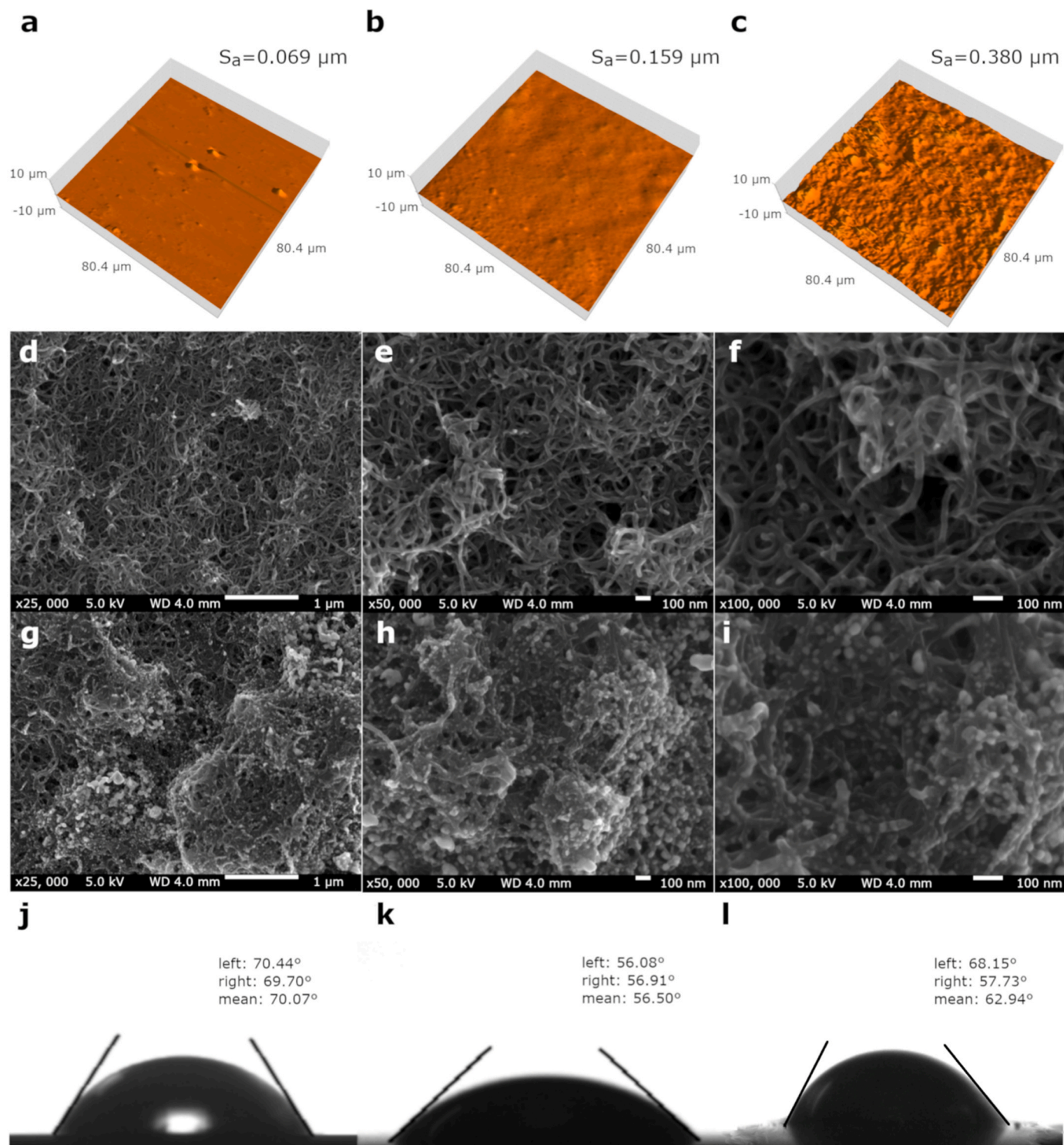


Fig. 1. The AFM-estimated S_a roughness for the MR (a), the MWCNTs coating (b), and the MWCNTs/Ag coating (c); the SEM surface topography for the MWCNTs coating (d, e, f) and the MWCNTs/Ag coating (g, h, i), and the CA results for the MR (j), the MWCNTs coating (k) and the MWCNTs/Ag coating (l).

platinum the counter-electrode, and a saturated calomel electrode (SCE) the reference electrode. The tests were performed in the Ringer's solution (in g L^{-1} : NaCl, 8.6; CaCl_2 , 0.33; KCl, 0.30) at a temperature of 37°C . The open circuit potential (OCP) was measured after 1 h and then the measurements were performed from -1.0 – 1.0 V at a scan rate of 1 mV s^{-1} .

3. Results

The surface roughness of MWCNTs coating increased after the deposition of the Ag NPs layer (Fig. 1 a-c). The Ag-formed agglomerates sized at $35 \pm 5.7 \text{ nm}$ were located on the edges and surface of the coatings. Each coating covered the substrate surface uniformly (Fig. 1 d-i).

In the wettability assessment, all surfaces were hydrophilic (Fig. 1 j-l). The Ag layer slightly increased the CA.

The EDS results for the MWCNTs/Ag coating (Fig. 2a) indicate the alloy elements, carbon from the MWCNTs, and silver. Some impurities, such as Cl and Si also appear. The Raman spectra of the MWCNTs/Ag coating (Fig. 2b) indicate the characteristic bands for the MWCNTs, such as the D band at 1375.5 cm^{-1} and G band at 1584.5 cm^{-1} [102], and less intense G' band at 2937 cm^{-1} also attributed to the [103]. The intensity ratio I_D/I_G , which informs about the degree of structural defecting, reached 0.48 for the MWCNTs/Ag coating.

The addition of Ag NPs brings out hardness H of $0.024 \pm 0.009 \text{ MPa}$, E of $3.06 \pm 0.74 \text{ GPa}$, and h_{max} of $4.29 \pm 0.80 \mu\text{m}$. Fig. 3a shows the comparison between PE and ERE characterizing the elastic and plastic properties. Young's modulus of the MWCNTs/Ag coating is 7-fold lower than for the MWCNTs layer (Fig. 3b). The MWCNTs/Ag coating demonstrates energy dissipated in the material higher than that released under the influence of tip load, thus it is almost 5-fold more plastic than the MWCNTs reference coating. The parameters such as the ratio of nanohardness to reduced Young's modulus (E/H_r) and the yield pressure (H^3/E_r^2) were also compared for the MWCNTs and MWCNTs/Ag coating (Fig. 3c-d) showing the MWCNTs/Ag coating is slightly more resistant to substrate deflections and thus coating chipping (Fig. 3c), and is 3-fold less resistant to plastic deformation under tip load (Fig. 3d). The observed L-D curves are shown in Fig. 4a-b.

Fig. 4c-d illustrates the relation of critical force (F_n) to critical friction (F_f) for each coating subjected to a nano-scratch test together with images of each scratch. The addition of Ag NPs to MWCNTs coating increased the L_c value to $57.74 \pm 3.03 \text{ mN}$, thus improving its adhesion

strength.

Fig. 5 shows the cross-section images of the MWCNTs and MWCNTs/Ag coating in two places with indicated coating thickness d . The MWCNTs and MWCNTs/Ag average coating thicknesses were, respectively, $3.58 \pm 0.84 \mu\text{m}$ and $5.26 \pm 0.31 \mu\text{m}$.

The results of corrosion tests are shown in Fig. 6. The MWCNTs coatings exhibit higher j_{corr} and E_{corr} values than the MR reference sample (Table 2), whereas the addition of the Ag NPs improved more than twice the corrosion resistance of the coating. It is to note a high OCP shift to anodic potentials for the MWCNTs coating.

4. Discussion

The EDS elementary analysis of the MWCNTs/Ag coating shows the presence of all anticipated elements, where picks attributed to silver clearly confirm the presence of this element in the coating. The Raman spectra show all characteristics of MWCNTs. The low I_D/I_G ratio in contrary to another report [104] can be attributed to the high degree of structural defects in the coating, decreased size and the number of sp^2 clusters, or the degree of functionalization [105]. In this case, FTIR spectroscopy is a better tool to show the presence of specific chemical bonds, such as Ag-O, which was reported in literature between 613 and 481 cm^{-1} [104].

The silver addition certainly increases the surface roughness of coatings. The silver agglomerates are sized at $35 \pm 5.7 \text{ nm}$ and located on the edges and surface of the carbon nanotubes as already observed [106]. Each MWCNTs coating covered evenly the substrate surface (Fig. 1 d-i). The previous results suggested the best osteoblast adhesion at a roughness R_a of 3 – $5 \mu\text{m}$ [107,108], but nanoroughness is also important [109]. In our previous publication for the coating composed of MWCNTs, Cu NPs, Ag NPs, and HAp, the achieved roughness was almost twice higher as here [40]. This difference can be attributed to the presence of HAp presumably increasing roughness as expected from ceramic coatings, but in each case, the roughness is acceptable for titanium implants.

The addition of Ag nanoparticles on the coating of MWCNTs resulted in a significant decrease in H and E values, and an increasing h_{max} (Table 3), calculated based on the L-D curves, revealing three stages of nanoindentation, observed previously [18]. Some earlier nanoindentation results [40,44] were added to the table to have a full spectrum of the results to discuss the effects.

The investigated coatings are softer than the four-component

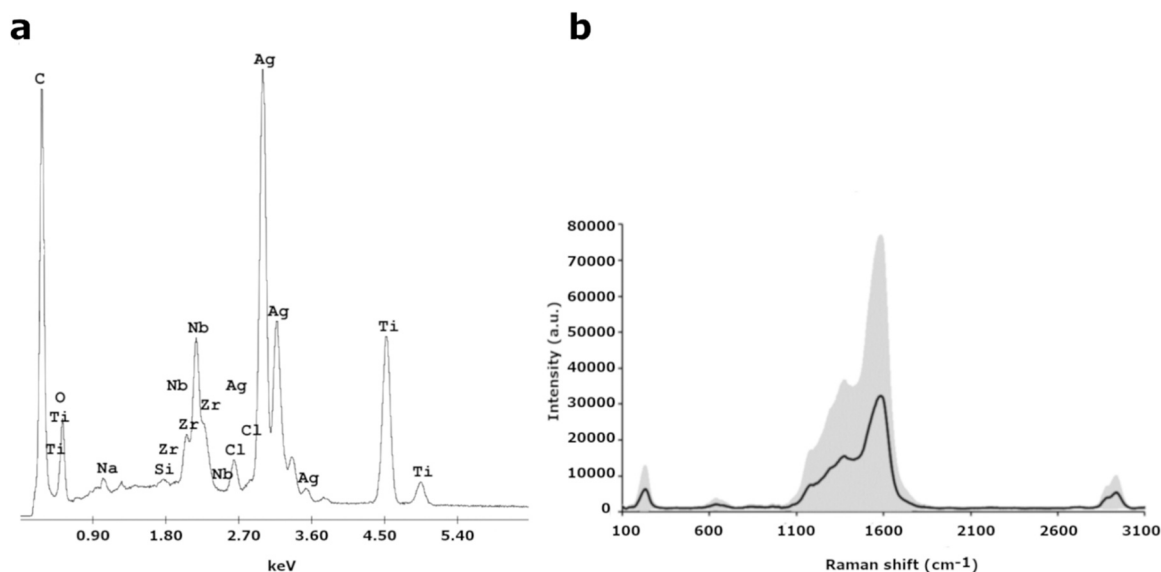


Fig. 2. The EDS (a) and Raman (b) spectra achieved for the MWCNTs/Ag coating.

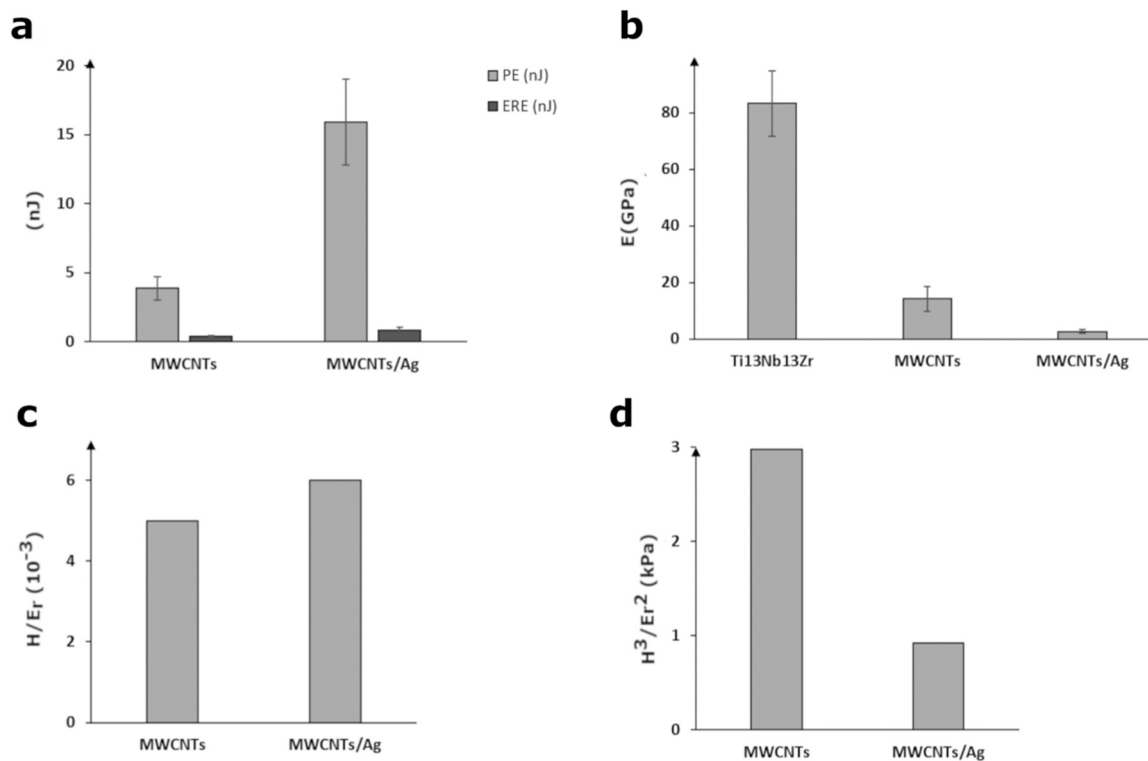


Fig. 3. The graphical comparison of nanoindentation test results between the tested materials: (a) PE and ERE, (b) E, (c), H/Er, and (d) H³/Er².

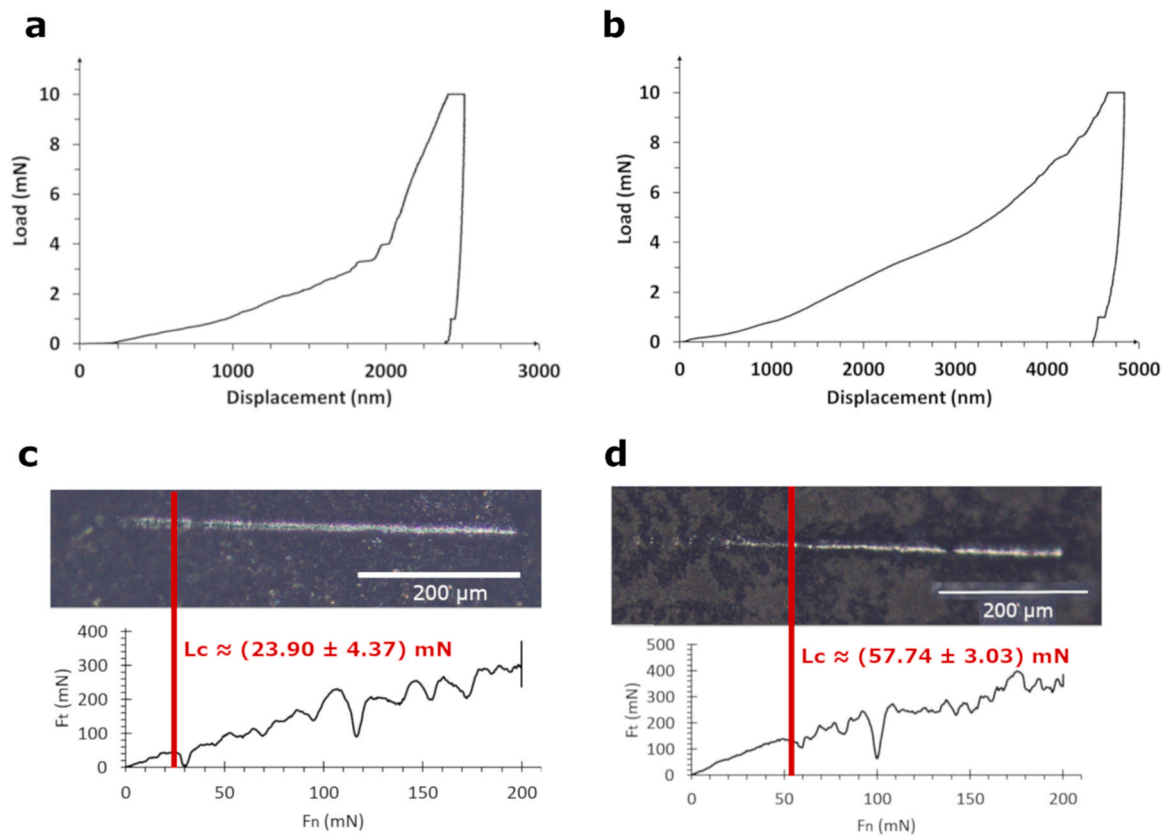


Fig. 4. The L-D curves and the nano-scratch test results with optical microscopy images of a specific scratch and indicated L_c for the MWCNTs coating (a, c) and the MWCNTs/Ag coating (b, d).

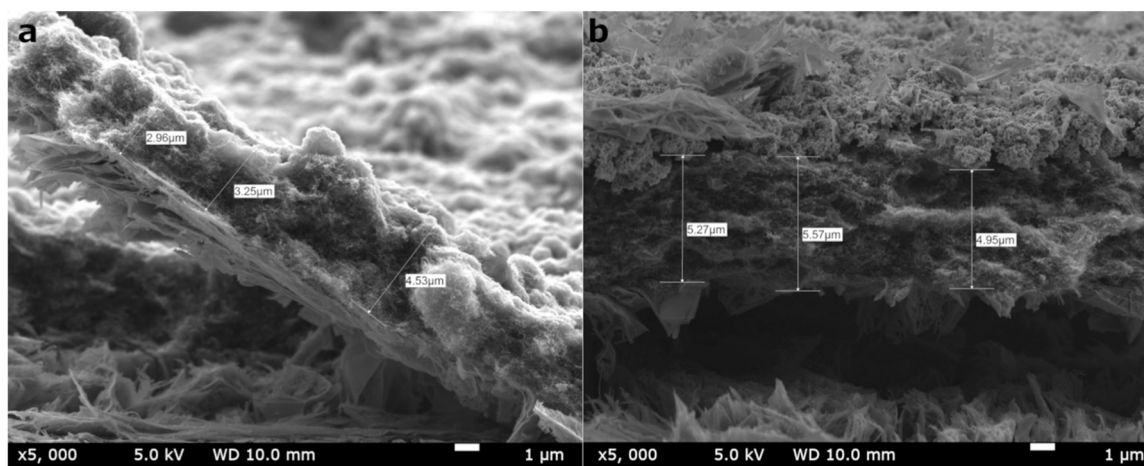


Fig. 5. Cross-sectional SEM images of the MWCNTs coating (a) and MWCNTs/Ag coating (b) with an indicated coating thickness.

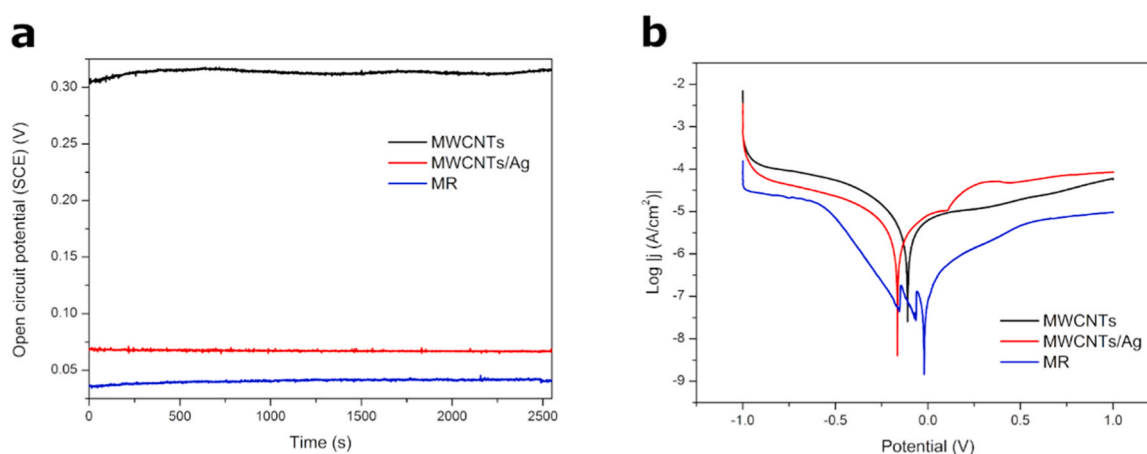


Fig. 6. The OCP vs. time (a) and potentiodynamic polarization curves for all tested samples (b).

Table 2

Corrosion test results for examined coatings.

Sample	E_{corr} (V (SCE))	j_{corr} (nA cm^{-2})
Ti13Nb13Zr	-0.019 ± 0.007	38.66 ± 5.92
MWCNTs	-0.109 ± 0.002	325.61 ± 33.61
MWCNTs/Ag	-0.165 ± 0.001	147.38 ± 13.73

MWCNTs-based tested previously, for them the H and E reached, respectively, 0.035 ± 0.019 GPa and 8.88 ± 3.26 GPa [40]. Moreover, the deposition of Ag NPs additionally decreases both parameters, presumably because silver aggregates are only physically adsorbed by MWCNTs and cannot resist indenter load.

The H/E and H^3/E^2 indexes can characterize elastic strain to failure, and resistance to plastic deformation. Comparing the other mechanical indexes here calculated with the previous ones [40], in which the H/E_r

Table 3

The nanoindentation results of the examined materials.

Sample	Nanohardness H (GPa)	Reduced Young's modulus E_r (GPa)	Surface Young's modulus E (GPa)	H/E _r (-)	H^3/E_r^2 (kPa)	Maximum indent depth (μm)
Ti13Nb13Zr	3.758 ± 1.045 *	116.91 ± 16.32 *	83.32 ± 11.63 *	0.032	3880	0.34 ± 0.037 *
MWCNTs	0.101 ± 0.049 *	18.59 ± 5.66 *	14.17 ± 4.32 *	0.005	2.98	2.07 ± 0.35 *
MWCNTs/Ag	0.024 ± 0.009	3.87 ± 0.94	3.06 ± 0.74	0.006	0.92	4.29 ± 0.80

* earlier results [40,44]

and H^3/E_r^2 values were, respectively, 0.003 and 0.31 kPa, the present coatings demonstrate improved behavior, likely because of a specific build-up of the coating. The slight increase of H/E_r and decrease of H^3/E_r^2 nanoindentation parameters may be the reason for the addition of the aggregated Ag NPs which are located on the MWCNTs walls, making it more plastic. Such a conclusion is by PE and ERE results: the first values, for the MWCNTs and MWCNTs/Ag, respectively, are 3.88 ± 0.85 nJ and 15.91 ± 3.12 nJ, and the second values, 0.38 ± 0.056 nJ and 0.85 ± 0.18 nJ (Fig. 3a), making the MWCNTs/Ag coating more plastic than the MWCNTs coating. However, the model describing the mechanical behavior of a complex composite structure of MWCNTs/Ag NPs coating cannot be proposed yet.

The coating adhesion was improved by the addition of Ag NPs achieving the highest L_c value. The adhesion determination by nano-scratch tests is infrequent, but here obtained values, 23.90 and 57.74 mN, are comparable to 12–45 mN observed for PEO-made ceramic

coatings on Mg-MWCNTs composite [110]. Whereas, the MWCNTs coatings in our previous research achieved different values for the MWCNTs and MWCNTs-based multicomponent coatings, respectively 89.42 ± 36.19 mN and 29.56 ± 6.92 mN [40]. The higher adhesion of previously developed bi-layer coating can be attributed, however, to higher h_{\max} and the more remarkable substrate influence.

In the wettability assessment, all surfaces were hydrophilic. The Ag layer slightly increased the CA, resulting in the values already observed for composite CNTs-Ag-based coatings [111,112] and proper for application in implantology. Compared to our previous research [40] the CA value for the MWCNTs-based coatings was much higher, 133° vs. 68° . The present wettability of the coating is then improved in terms of biomedical applications, presumably because of plausible surface architecture, in which the presence of silver agglomerates only slightly decreases the hydrophilicity.

The results of corrosion tests are shown in Fig. 6. All the OCP values were positive due to surface passivation. The MWCNTs coatings exhibit higher j_{corr} and E_{corr} values than the MR sample, thus weakening the corrosion resistance of the Ti13Nb13Zr alloy (Table 2). The porous and fibrous structure lowers the corrosion resistance of titanium [113] and the presence of Ag NPs improves this behavior, likely by decreasing the porosity. On the other side, here the CNTs coatings decreased the corrosion current density, adversely to the substantial improvement in corrosion resistance reported in [114], attributed to their chemical inertness. Again, the architectural features such as porosity and components of coatings play an important role. As concerns the silver addition, its positive effect was already observed for polypyrrole coating on titanium [115] and is considered as the effect of better passivation. We think that the major cause of the corrosion behavior of CNTs-Ag coating is better than CNTs alone is followed by its sealing by nanoparticles of noble metal and decreasing porosity. Comparing this result to other coatings deposited on hydroxyapatite coatings on titanium, as recently strontium doped HAp [84,116], HAp coating is certainly more dense and less permeable for ions than HAp. Therefore, in future research, either anodic oxidation, or an elevation of Ag NPs amount, or including into the coating of the chemical compound sealing the pores research.

Summarizing the results it can be concluded that the addition of Ag NPs even in high amounts improves only some coating features. In particular, the increasing adhesion is still not quite enough and an addition of either a sub-layer or a component strongly coherent to both titanium and CNTs, or the mechanical/chemical preliminary surface treatment, or reinforcement of CNTs network with oxide particles, or EPD of silver at much higher voltage and time can be considered, investigated and developed. The small hardness and resistance to plastic deformation are acceptable or even desired taking into account the high loads carried on implants during their placement in the body. The advantages are high corrosion resistance and wettability of Ag-doped CNTs coatings.

5. Conclusions

The coating composed of the MWCNTs layer decorated with the Ag NPs layer demonstrates the surface roughness in a nanoscale range which can be accepted for medical applications. The relatively low mechanical properties of MWCNTs/Ag coating result from the loose MWCNTs layer structure and the penetration of the inner layer by Ag NPs only physically adsorbed on CNTs. The difference in adhesion of both coatings might be caused by the bare metal effect. The increased corrosion resistance compared to the MWCNTs base coating is likely produced by decreasing penetration of the layer by Ag NPs.

Funding

This research did not receive any specific grant from funding agencies in the public, commercial, or not-for-profit sectors.

CRedit authorship contribution statement

Dorota Rogala-Wielgus: Conceptualization, Methodology, Data curation, Visualization, Investigation, Formal analysis, Roles/Writing - original draft; **Beata Majkowska-Marzec:** Methodology, Visualization, Project administration; **Andrzej Zielinski:** Supervision, Writing - review & editing.

Declaration of Competing Interest

The authors declare that they have no known competing financial interests or personal relationships that could have appeared to influence the work reported in this paper.

Data availability

Data will be made available on request.

Acknowledgments

We are grateful to Dr. Grzegorz Gajowicz and Malwina Liszewska for their support in the evaluation of the results.

References

- [1] P. Jiang, Y. Zhang, R. Hu, B. Shi, L. Zhang, Q. Huang, Y. Yang, P. Tang, C. Lin, Advanced surface engineering of titanium materials for biomedical applications: from static modification to dynamic responsive regulation, *Bioact. Mater.* 27 (2023) 15–57, <https://doi.org/10.1016/j.bioactmat.2023.03.006>.
- [2] B. Makurat-Kasprolewicz, A. Ossowska, Recent advances in electrochemically surface treated titanium and its alloys for biomedical applications: a review of anodic and plasma electrolytic oxidation methods, *Mater. Today Commun.* 34 (2023), 105425, <https://doi.org/10.1016/j.mtcomm.2023.105425>.
- [3] X. Han, J. Ma, A. Tian, Y. Wang, Y. Li, B. Dong, X. Tong, X. Ma, Surface modification techniques of titanium and titanium alloys for biomedical orthopaedics applications: a review, *Colloids Surf. B Biointerfaces* 227 (2023), 113339, <https://doi.org/10.1016/j.colsurfb.2023.113339>.
- [4] S. Chowdhury, N. Arunachalam, Surface functionalization of additively manufactured titanium alloy for orthopaedic implant applications, *J. Manuf. Process.* 102 (2023) 387–405, <https://doi.org/10.1016/j.jmapro.2023.07.015>.
- [5] J.C.M. Souza, M.B. Sordi, M. Kanazawa, S. Ravindran, B. Henriques, F.S. Silva, C. Aparicio, L.F. Cooper, Nano-scale modification of titanium implant surfaces to enhance osseointegration, *Acta Biomater.* 94 (2019) 112–131, <https://doi.org/10.1016/j.actbio.2019.05.045>.
- [6] R.C. Costa, B.E. Nagay, C. Dini, M.H.R. Borges, L.F.B. Miranda, J.M. Cordeiro, J. G.S. Souza, C. Sukotjo, N.C. Cruz, V.A.R. Barão, The race for the optimal antimicrobial surface: perspectives and challenges related to plasma electrolytic oxidation coating for titanium-based implants, *Adv. Colloid Interface Sci.* 311 (2023), 102805, <https://doi.org/10.1016/j.cis.2022.102805>.
- [7] Z. Yuan, Y. He, C. Lin, P. Liu, K. Cai, Antibacterial surface design of biomedical titanium materials for orthopedic applications, *J. Mater. Sci. Technol.* 78 (2021) 51–67, <https://doi.org/10.1016/j.jmst.2020.10.066>.
- [8] H. Chourifa, H. Bouloussa, V. Mignonney, C. Falentin-Daudré, Review of titanium surface modification techniques and coatings for antibacterial applications, *Acta Biomater.* 83 (2019) 37–54, <https://doi.org/10.1016/j.actbio.2018.10.036>.
- [9] J. Quinn, R. Mcfadden, C.-W. Chan, L. Carson, *Titanium for Orthopedic Applications: an Overview of Surface Modification to Improve Biocompatibility and Prevent Bacterial Biofilm Formation*, *Isci* 23 (2020) <https://doi.org/10.1016/j.isci.2020.101745>.
- [10] L.M. Pandey, Design of biocompatible and self-antibacterial titanium surfaces for biomedical applications, *Curr. Opin. Biomed. Eng.* 25 (2023), 100423, <https://doi.org/10.1016/j.cobme.2022.100423>.
- [11] S. Wang, X. Zhao, Y. Hsu, Y. He, F. Wang, F. Yang, F. Yan, D. Xia, Y. Liu, Surface modification of titanium implants with Mg-containing coatings to promote osseointegration, *Acta Biomater.* 169 (2023) 19–44, <https://doi.org/10.1016/j.actbio.2023.07.048>.
- [12] S. Malathi, I. Pakrudheen, S.N. Kalkura, T.J. Webster, S. Balasubramanian, Disposable biosensors based on metal nanoparticles, *Sens. Int.* 3 (2022), 100169, <https://doi.org/10.1016/j.sintl.2022.100169>.
- [13] D.A. Ali, M.M. Mehanna, Role of lignin-based nanoparticles in anticancer drug delivery and bioimaging: an up-to-date review, *Int. J. Biol. Macromol.* 221 (2022) 934–953, <https://doi.org/10.1016/j.ijbiomac.2022.09.007>.
- [14] Q. Xu, F. Xiao, H. Xu, Fluorescent detection of emerging virus based on nanoparticles: from synthesis to application, *TrAC, Trends Anal. Chem.* 161 (2023), 116999, <https://doi.org/10.1016/j.trac.2023.116999>.
- [15] S. Zhang, J. Bai, W. Kong, H. Song, Y. Liu, G. Liu, L. Ma, L. Zhou, Y. Jiang, Dendritic mesoporous silica nanoparticles for enzyme immobilization (in press.), *Green. Chem. Eng.* (2023), <https://doi.org/10.1016/j.gce.2023.07.002>.

- [16] N. Hossain, M.H. Mobarak, M.A. Mimona, M.A. Islam, A. Hossain, F.T. Zohura, M. A. Chowdhury, Advances and significances of nanoparticles in semiconductor applications – A review, *Results Eng.* 19 (2023), 101347, <https://doi.org/10.1016/j.rineng.2023.101347>.
- [17] S. Shenoy, K. Sridharan, A robust photocatalyst using silver quantum clusters grafted in titanium dioxide nanotubes, *Surf. Interfaces* 30 (2022), 101941, <https://doi.org/10.1016/j.surfin.2022.101941>.
- [18] W. Ma, X. Zhang, Study of the thermal, electrical and thermoelectric properties of metallic nanofilms, *Int. J. Heat. Mass Transf.* 58 (2013) 639–651, <https://doi.org/10.1016/j.ijheatmasstransfer.2012.11.025>.
- [19] N.D. Hai, N.M. Dat, N.T.H. Nam, H. An, L.T. Tai, L.M. Huong, C.Q. Cong, N.T. H. Giang, N.T. Tinh, N.H. Hieu, A review on the chemical and biological synthesis of silver nanoparticles/graphene oxide nanocomposites: a comparison, *Mater. Today Sustain.* 24 (2023), 100544, <https://doi.org/10.1016/j.mtsust.2023.100544>.
- [20] Z. Wang, S. Liang, Y. Kang, W. Zhao, Y. Xia, J. Yang, H. Wang, X. Zhang, Manipulating interfacial polymerization for polymeric nanofilms of composite separation membranes, *Prog. Polym. Sci.* 122 (2021), 101450, <https://doi.org/10.1016/j.progpolymsci.2021.101450>.
- [21] S. Ali, X. Chen, S. Ahmad, W. Shah, M. Shafique, P. Chaubey, G. Mustafa, A. Alrashidi, S. Alharthi, Advancements and challenges in phytochemical-mediated silver nanoparticles for food packaging: recent review (2021–2023), *Trends Food Sci. Technol.* 141 (2023), 104197, <https://doi.org/10.1016/j.tifs.2023.104197>.
- [22] R.H. Althomali, W.A. Adeosun, Wet chemically synthesized metal oxides nanoparticles, characterization and application in electrochemical energy storage: an updated review, *Synth. Met.* 298 (2023), 117424, <https://doi.org/10.1016/j.synthmet.2023.117424>.
- [23] M. Rafiq, R.S. Khan, A.H. Rather, T.U. Wani, A. Qureshi, A.H. Pandith, S. Rather, F.A. Sheikh, Overview of printable nanoparticles through inkjet process: their application towards medical use, *Microelectron. Eng.* 266 (2022), 111889, <https://doi.org/10.1016/j.mee.2022.111889>.
- [24] S. Rathinavel, K. Priyadarshini, D. Panda, A review on carbon nanotube: an overview of synthesis, properties, functionalization, characterization, and the application, *Mater. Sci. Eng.:B* 268 (2021), 115095, <https://doi.org/10.1016/j.mseb.2021.115095>.
- [25] N. Manikandan, V.P. Suresh Kumar, S. Siva Murugan, G. Rathi, K. Vishnu Saran, T.K. Shabariganesh, Carbon nanotubes and their properties-The review, *Mater. Today Proc.* 47 (2021) 4682–4685, <https://doi.org/10.1016/j.matpr.2021.05.543>.
- [26] J.-E. Park, Y.-S. Jang, T.-S. Bae, M.-H. Lee, Biocompatibility Characteristics of Titanium Coated with Multi Walled Carbon Nanotubes—Hydroxyapatite Nanocomposites, *Mater* 12 (2019) 224, <https://doi.org/10.3390/ma12020224>.
- [27] X. Ji, X. Li, H. Yu, W. Zhang, H. Dong, Study on the carbon nanotubes reinforced nanocomposite coatings, *Diam. Relat. Mater.* 91 (2019) 247–254, <https://doi.org/10.1016/j.diamond.2018.11.027>.
- [28] N. Anzar, R. Hasan, M. Tyagi, N. Yadav, J. Narang, Carbon nanotube - A review on Synthesis, Properties and plethora of applications in the field of biomedical science, *Sens. Int.* 1 (2020), 100003, <https://doi.org/10.1016/j.sintl.2020.100003>.
- [29] S.A. Mezzasalma, L. Grassi, M. Grassi, Physical and chemical properties of carbon nanotubes in view of mechanistic neuroscience investigations. Some outlook from condensed matter, materials science and physical chemistry, *Mater. Sci. Eng. C* 131 (2021), 112480, <https://doi.org/10.1016/j.msec.2021.112480>.
- [30] B.O. Murjani, P.S. Kadu, M. Bansod, S.S. Vaidya, M.D. Yadav, Carbon nanotubes in biomedical applications: current status, promises, and challenges, *Carbon Lett.* 32 (2022) 1207–1226, <https://doi.org/10.1007/s42823-022-00364-4>.
- [31] C. Caoduro, E. Hervouet, C. Girard-Thernier, T. Gharbi, H. Boulahdour, R. Delage-Mourroux, M. Pudlo, Carbon nanotubes as gene carriers: focus on internalization pathways related to functionalization and properties, *Acta Biomater.* 49 (2017) 36–44, <https://doi.org/10.1016/j.actbio.2016.11.013>.
- [32] M.M. Farag, Recent trends on biomaterials for tissue regeneration applications: review, *J. Mater. Sci.* 58 (2023) 527–558, <https://doi.org/10.1007/s10853-022-08102-x>.
- [33] A. Zieliński, B. Majkowska-Marzec, Whether Carbon Nanotubes Are Capable, Promising, and Safe for Their Application in Nervous System Regeneration. Some Critical Remarks and Research Strategies, *Coat* 12 (2022) 1643, <https://doi.org/10.3390/coatings12111643>.
- [34] K. Stenberg, S. Ditttrick, S. Bose, A. Bandyopadhyay, Influence of simultaneous addition of carbon nanotubes and calcium phosphate on wear resistance of 3D-printed Ti6Al4V, *J. Mater. Res.* 33 (2018) 2077–2086, <https://doi.org/10.1557/jmr.2018.234>.
- [35] A. Weselucha-Birczyńska, E. Stodolak-Zych, W. Piś, E. Długoń, A. Benko, M. Błażewicz, A model of adsorption of albumin on the implant surface titanium and titanium modified carbon coatings (MWCNT-EPD). 2D correlation analysis, *J. Mol. Struct.* 1124 (2016) 61–70, <https://doi.org/10.1016/j.molstruc.2016.04.050>.
- [36] J. Deng, S. Pang, C. Wang, T. Ren, Biotribological properties of Ti-6Al-4V alloy treated with self-assembly multi-walled carbon nanotube coating, *Surf. Coat. Technol.* 382 (2020), 125169, <https://doi.org/10.1016/j.surfcoat.2019.125169>.
- [37] D. Gopi, E. Shinyjoy, M. Sekar, M. Surendiran, L. Kavitha, T.S. Sampath Kumar, Development of carbon nanotubes reinforced hydroxyapatite composite coatings on titanium by electrodeposition method, *Corros. Sci.* 73 (2013) 321–330, <https://doi.org/10.1016/j.corsci.2013.04.021>.
- [38] X. Pei, Y. Zeng, R. He, Z. Li, L. Tian, J. Wang, Q. Wan, X. Li, H. Bao, Single-walled carbon nanotubes/hydroxyapatite coatings on titanium obtained by electrochemical deposition, *Appl. Surf. Sci.* 295 (2014) 71–80, <https://doi.org/10.1016/j.apsusc.2014.01.009>.
- [39] S. Devgan, S.S. Sidhu, Surface modification of β -type titanium with multi-walled CNTs/ μ -HAP powder mixed Electro Discharge Treatment process, *Mater. Chem. Phys.* 239 (2020), 122005, <https://doi.org/10.1016/j.matchemphys.2019.122005>.
- [40] Majkowska-Marzec, Rogala-Wielgus, Bartmański, Bartosewicz, Zieliński, Comparison of Properties of the Hybrid and Bilayer MWCNTs—Hydroxyapatite Coatings on Ti Alloy, *Coat* 9 (2019) 643, <https://doi.org/10.3390/coatings9100643>.
- [41] B. Chen, X. Li, Y. Jia, L. Xu, H. Liang, X. Li, J. Yang, C. Li, F. Yan, Fabrication of ternary hybrid of carbon nanotubes/graphene oxide/MoS₂ and its enhancement on the tribological properties of epoxy composite coatings, *Compos. Part A Appl. Sci. Manuf.* 115 (2018) 157–165, <https://doi.org/10.1016/j.compositesa.2018.09.021>.
- [42] H. Maleki-Ghaleh, J. Khalil-Allafi, Characterization, mechanical and in vitro biological behavior of hydroxyapatite-titanium-carbon nanotube composite coatings deposited on NiTi alloy by electrophoretic deposition, *Surf. Coat. Technol.* 363 (2019) 179–190, <https://doi.org/10.1016/j.surfcoat.2019.02.029>.
- [43] D. Rogala-Wielgus, B. Majkowska-Marzec, A. Zieliński, B.J. Jankiewicz, Mechanical Behavior of Bi-Layer and Dispersion Coatings Composed of Several Nanostructures on Ti Substrate, *Appl. Sci.* 11 (2021) 7862, <https://doi.org/10.3390/app11177862>.
- [44] D. Rogala-Wielgus, B. Majkowska-Marzec, A. Zieliński, M. Bartmański, B. Bartosewicz, Mechanical Behavior of Bi-Layer and Dispersion Coatings Composed of Several Nanostructures on Ti3Nb13Zr Alloy, *Mater* 14 (2021) 2905, <https://doi.org/10.3390/ma14112905>.
- [45] M.A. Gizawy, H.A. Shamsel-Din, I.M. Abdelmonem, M.I.A. Ibrahim, L. A. Mohamed, E. Metwally, Synthesis of chitosan-acrylic acid/multiwalled carbon nanotubes composite for theranostic 47Sc separation from neutron irradiated titanium target, *Int. J. Biol. Macromol.* 163 (2020) 79–86, <https://doi.org/10.1016/j.ijbiomac.2020.06.249>.
- [46] J. Marchewka, P. Jeleń, E. Długoń, M. Sitarz, M. Błażewicz, Spectroscopic investigation of the carbon nanotubes and polysiloxane coatings on titanium surface, *J. Mol. Struct.* 1212 (2020), 128176, <https://doi.org/10.1016/j.molstruc.2020.128176>.
- [47] Z. Ye, J. Li, L. Liu, F. Ma, B. Zhao, X. Wang, Microstructure and wear performance enhancement of carbon nanotubes reinforced composite coatings fabricated by laser cladding on titanium alloy, *Opt. Laser Technol.* 139 (2021), 106957, <https://doi.org/10.1016/j.optlastec.2021.106957>.
- [48] S. Vahedi, R.M. Aghdam, M.H. Sohi, A.H. Rezaian, Characteristics of electrospun chitosan/carbon nanotube coatings deposited on AZ31 magnesium alloy, *J. Mater. Sci. Mater. Med.* 34 (2023), 8, <https://doi.org/10.1007/s10856-022-06703-1>.
- [49] A. Dhaka, S. Chand Mali, S. Sharma, R. Trivedi, A review on biological synthesis of silver nanoparticles and their potential applications, *Results Chem.* 6 (2023), 101108, <https://doi.org/10.1016/j.rechem.2023.101108>.
- [50] A. Peter, S. Sadanandan, E.S. Bindiya, N. Mohan, S.G. Bhat, K. Abhitha, Biofilm inhibition on natural rubber by hydrophilic modification using carboxymethyl chitosan stabilised high energy faceted silver nanoparticles, *Carbohydr. Polym. Technol. Appl.* 6 (2023), 100357, <https://doi.org/10.1016/j.carpta.2023.100357>.
- [51] B. Wang, Z. Wu, J. Lan, Y. Li, L. Xie, X. Huang, A. Zhang, H. Qiao, X. Chang, H. Lin, H. Ag, co-functionalized strontium titanate nanotubes for inhibition of bacterial-associated infection and enhancement of in vivo osseointegration, *Surf. Coat. Technol.* 405 (2021), 126700, <https://doi.org/10.1016/j.surfcoat.2020.126700>.
- [52] A. Perumal, S. Kannan, R. Nallaiyan, Silver nanoparticles incorporated polyaniline on TiO₂ nanotube arrays: a nanocomposite platform to enhance the biocompatibility and antibiofilm, *Surf. Interfaces* 22 (2021), 100892, <https://doi.org/10.1016/j.surfin.2020.100892>.
- [53] N.M. Mwenze, M. Juma, M. Maaza, Z. Birech, M.S. Dhlamini, Laser liquid ablation for silver nanoparticles synthesis and conjugation with hydroxychloroquine for Covid-19 treatment (in press.), *Mater. Today Proc.* (2023), <https://doi.org/10.1016/j.matpr.2023.08.195>.
- [54] M. Stoian, A. Kuncser, F. Neatu, M. Florea, M. Popa, S.N. Voicu, M.C. Chifiriuc, A. Hanganu, M.E. Anghel, M. Tudose, Green synthesis of aminated hyaluronic acid-based silver nanoparticles on modified titanium dioxide surface: influence of size and chemical composition on their biological properties, *Int. J. Biol. Macromol.* 253 (2023), 127445, <https://doi.org/10.1016/j.ijbiomac.2023.127445>.
- [55] G. Karabulut, N. Beköz Üllen, E. Akyüz, S. Karakuş, Surface modification of 316L stainless steel with multifunctional locust gum/polyethylene glycol-silver nanoparticles using different coating methods, *Prog. Org. Coat.* 174 (2023), 107291, <https://doi.org/10.1016/j.porgcoat.2022.107291>.
- [56] L. Pawłowski, M. Bartmański, A. Mielewczyk-Gryń, A. Zieliński, Chitosan/poly(4-vinylpyridine) coatings formed on AgNPs-decorated titanium, *Mater. Lett.* 319 (2022), 132293, <https://doi.org/10.1016/j.matlet.2022.132293>.
- [57] L. Pawłowski, M. Asim Akhtar, A. Zieliński, A.R. Boccaccini, Biological properties of chitosan/Eudragit E 100 and chitosan/poly(4-vinylpyridine) coatings electrochemically deposited on AgNPs-decorated titanium substrate, *Mater. Lett.* 336 (2023), 133885, <https://doi.org/10.1016/j.matlet.2023.133885>.
- [58] L. Pawłowski, J. Wawrzyniak, A. Banach-Kopec, B.M. Cieślak, K. Jurak, J. Karczewski, R. Tylingo, K. Siuzdak, A. Zieliński, Antibacterial properties of laser-encapsulated titanium oxide nanotubes decorated with nanosilver and

- covered with chitosan/Eudragit polymers, *Biomater. Adv.* 138 (2022), 212950, <https://doi.org/10.1016/j.bioadv.2022.212950>.
- [59] M.S. Tawakal, A.M. Abdelghany Metwally, N.A. El-Wassefy, M.A. Tawfik, M. S. Shamaa, Static friction, surface roughness, and antibacterial activity of orthodontic brackets coated with silver and silver chitosan nanoparticles (in press.), *J. World Fed. Orthod.* (2023), <https://doi.org/10.1016/j.ejwf.2023.08.002>.
- [60] H. Waqas, U. Farooq, D. Liu, M. Alghamdi, S. Noreen, T. Muhammad, Numerical investigation of nanofluid flow with gold and silver nanoparticles injected inside a stenotic artery, *Mater. Des.* 223 (2022), 111130, <https://doi.org/10.1016/j.matdes.2022.111130>.
- [61] J. Gaviria, A. Alcudia, B. Begines, A.M. Beltrán, J. Villarraga, R. Moriche, J. A. Rodríguez-Ortiz, Y. Torres, Synthesis and deposition of silver nanoparticles on porous titanium substrates for biomedical applications, *Surf. Coat. Technol.* 406 (2021), 126667, <https://doi.org/10.1016/j.surfcoat.2020.126667>.
- [62] A. Damlé, R. Sundaresan, J.M. Rajwade, P. Srivastava, A. Naik, A concise review on implications of silver nanoparticles in bone tissue engineering, *Biomater. Adv.* 141 (2022), 213099, <https://doi.org/10.1016/j.bioadv.2022.213099>.
- [63] N. Xu, T. Zhang, X. Wang, L. Wang, Cardioprotective effects of plant-based silver nanoparticles: describing a modern drug, *Inorg. Chem. Commun.* 158 (2023), 111525, <https://doi.org/10.1016/j.inoche.2023.111525>.
- [64] B. Arul, R. Kothai, Biosynthesis, in-vitro antioxidant and cytotoxic potential of silver nanoparticles of *Abutilon hirtum* (Lamp) Sweet (in press.), *Mater. Today Proc.* (2023), <https://doi.org/10.1016/j.matpr.2023.08.009>.
- [65] A. Zandvakili, M. Moradi, P. Ashoo, R. Pournejati, R. Yosefi, H.R. Karbalaei-Heidari, S. Behaain, Investigating cytotoxicity effect of Ag- deposited, doped and coated titanium dioxide nanotubes on breast cancer cells, *Mater. Today Commun.* 32 (2022), 103915, <https://doi.org/10.1016/j.mtcomm.2022.103915>.
- [66] A. Balasubramanian, K. Ramalingam, In-vivo anticancer activity of biosynthetic silver nanoparticles of *Cassia marginata* Roxb against NMU-Induced mammary carcinoma (in press.), *Mater. Today Proc.* (2023), <https://doi.org/10.1016/j.matpr.2023.07.011>.
- [67] K. Krishnamoorthy, S. Jayaraman, R. Krishnamoorthy, S. Manoharadas, M. A. Alshuniaber, B. Vikas, V. Priya Veeraraghavan, Green synthesis and evaluation of anti-microbial, antioxidant, anti-inflammatory, and anti-diabetic activities of silver nanoparticles from *Argyrea nervosa* leaf extract: an invitro study, *J. King Saud. Univ. -Sci.* 35 (2023), 102955, <https://doi.org/10.1016/j.jksus.2023.102955>.
- [68] S. Maheshwari, Synergistic effects of *Woodfordia fruticosa* silver nanoparticles accelerating wound healing in Swiss mice in vivo (in press.), *Intell. Pharm.* (2023), <https://doi.org/10.1016/j.iphpa.2023.09.005>.
- [69] F. Qiu, H. Lu, X. Wang, Y. Yang, M. Ding, Evaluation of the nephroprotective properties of silver nanoparticles green-mediated by arabic gum on the lipopolysaccharide-induced acute kidney injury, *Inorg. Chem. Commun.* 155 (2023), 111043, <https://doi.org/10.1016/j.inoche.2023.111043>.
- [70] R.S.A. Hameed, S. Obeidat, M.T. Qureshi, S.R. Al-Mhyawi, E.H. Aljuhani, M. Abdallah, Silver nanoparticles – Expired medicinal drugs waste accumulated at hail city for the local manufacturing of green corrosion inhibitor system for steel in acidic environment, *J. Mater. Res. Technol.* 21 (2022) 2743–2756, <https://doi.org/10.1016/j.jmrt.2022.10.081>.
- [71] S.R. Al-Mhyawi, Green synthesis of silver nanoparticles and their inhibitory efficacy on corrosion of carbon steel in hydrochloric acid solution, *Int. J. Electrochem. Sci.* 18 (2023), 100210, <https://doi.org/10.1016/j.ijoes.2023.100210>.
- [72] N. Raghavendra, R.T. Mahesh, B. Mahanthesh, J. Mackolil, Optimization of anti-corrosion performance of novel magnetic polyaniline-Chitosan nanocomposite decorated with silver nanoparticles on Al in simulated acidizing environment using RSM, *Int. J. Biol. Macromol.* 195 (2022) 329–345, <https://doi.org/10.1016/j.ijbiomac.2021.11.207>.
- [73] E. Ituen, A. Singh, L. Yuanhua, O. Akaranta, Biomass-mediated synthesis of silver nanoparticles composite and application as green corrosion inhibitor in oilfield acidic cleaning fluid, *Clean. Eng. Technol.* 3 (2021), 100119, <https://doi.org/10.1016/j.clet.2021.100119>.
- [74] M. Ali Asaad, P. Bothi Raja, G. Fahim Huseien, R. Fediuk, M. Ismail, R. Alyousef, Self-healing epoxy coating doped with *Elaeis guineensis*/silver nanoparticles: a robust corrosion inhibitor, *Constr. Build. Mater.* 312 (2021), 125396, <https://doi.org/10.1016/j.conbuildmat.2021.125396>.
- [75] C. Chen, W. Li, X. Liu, J. Yu, S. Xing, J. Yang, Q. Han, Silver nanoparticles/graphene oxide arranged on polytetrafluoroethylene substrate hydrophilic modified with TiO₂ to construct efficient air purification material, *J. Environ. Chem. Eng.* 11 (2023), 110848, <https://doi.org/10.1016/j.jece.2023.110848>.
- [76] V.-D. Doan, V.T. Le, D.L. Tran, T.L.H. Nguyen, D.C. Nguyen, A.-T. Nguyen, V. T. Le, Catalytic reduction of nitrophenols using *Gnetum montanum* extract capped silver nanoparticles, *Mol. Catal.* 534 (2023), 112804, <https://doi.org/10.1016/j.mcat.2022.112804>.
- [77] E. Naderi-Samani, R.S. Razavi, K. Nekouee, H. Naderi-Samani, Synthesis of silver nanoparticles for use in conductive inks by chemical reduction method, *Heliyon* 9 (2023), e20548, <https://doi.org/10.1016/j.heliyon.2023.e20548>.
- [78] B.-J. Kim, J.-S. Park, Y.-J. Hwang, J.-S. Park, Characteristics of silver meshes coated with carbon nanotubes via spray-coating and electrophoretic deposition for touch screen panels, *Thin Solid Films* 596 (2015) 68–71, <https://doi.org/10.1016/j.tsf.2015.07.084>.
- [79] Y. Shao, Y. Luan, C. Hao, J. Song, L. Li, F. Song, Antimicrobial protection of two controlled release silver nanoparticles on simulated silk cultural relic, *J. Colloid Interface Sci.* 652 (2023) 901–911, <https://doi.org/10.1016/j.jcis.2023.08.116>.
- [80] X. Ji, X. Li, H. Yu, W. Zhang, H. Dong, Study on the carbon nanotubes reinforced nanocomposite coatings, *Diam. Relat. Mater.* 91 (2019) 247–254, <https://doi.org/10.1016/j.diamond.2018.11.027>.
- [81] D.-E. Kim, C.-L. Kim, H.-J. Kim, A novel approach to wear reduction of micro-components by synthesis of carbon nanotube-silver composite coating, *CIRP Ann.* 60 (2011) 599–602, <https://doi.org/10.1016/j.cirp.2011.03.014>.
- [82] N. Hintsho, L. Petrik, A. Nechaev, S. Titinchi, P. Ndungu, Photo-catalytic activity of titanium dioxide carbon nanotube nano-composites modified with silver and palladium nanoparticles, *Appl. Catal. B* 156–157 (2014) 273–283, <https://doi.org/10.1016/j.apcatb.2014.03.021>.
- [83] B. Wang, J. Lan, H. Qiao, L. Xie, H. Yang, H. Lin, X. Li, Y. Huang, Porous surface with fusion peptides embedded in strontium titanate nanotubes elevates osteogenic and antibacterial activity of additively manufactured titanium alloy, *Colloids Surf. B Biointerfaces* 224 (2023), 113188, <https://doi.org/10.1016/j.colsurf.2023.113188>.
- [84] B. Wang, A. Bian, F. Jia, J. Lan, H. Yang, K. Yan, L. Xie, H. Qiao, X. Chang, H. Lin, H. Zhang, Y. Huang, Dual-functional[†] strontium titanate nanotubes designed based on fusion peptides simultaneously enhancing anti-infection and osseointegration, *Biomater. Adv.* 133 (2022), 112650, <https://doi.org/10.1016/j.msec.2022.112650>.
- [85] B. Wang, Z. Wu, S. Wang, S. Wang, Q. Niu, Y. Wu, F. Jia, A. Bian, L. Xie, H. Qiao, X. Chang, H. Lin, H. Zhang, Y. Huang, Mg/Cu-doped TiO₂ nanotube array: a novel dual-function system with self-antibacterial activity and excellent cell compatibility, *Mater. Sci. Eng. C* 128 (2021), 112322, <https://doi.org/10.1016/j.msec.2021.112322>.
- [86] N. Roy, A. Ejaz, S.W. Joo, S. Jeon, Aligned silver nanoparticles anchored on pyrrolic and pyridinic-nitrogen induced carbon nanotubes for enhanced oxygen reduction reaction, *Thin Solid Films* 769 (2023), 139710, <https://doi.org/10.1016/j.tsf.2023.139710>.
- [87] D.U. Bahar, C. Topcu, D. Ozcimen, I. Isildak, A Novel Borate Ion Selective Electrode Based On Carbon Nanotube-Silver Borate, *Int. J. Electrochem. Sci.* 15 (2020) 899–914, <https://doi.org/10.20964/2020.01.40>.
- [88] G. Yang, R. Wang, D. Fang, T. Hu, C. Bao, J. Yi, Nano-silver modified carbon nanotubes to reinforce the copper matrix composites and their mechanical properties, *Adv. Powder Technol.* 33 (2022), 103672, <https://doi.org/10.1016/j.apt.2022.103672>.
- [89] M.S. Islam, A.N. Naz, M.N. Alam, A.K. Das, J.H. Yeum, Electrospun poly(vinyl alcohol)/silver nanoparticle/carbon nanotube multi-composite nanofiber mat: fabrication, characterization and evaluation of thermal, mechanical and antibacterial properties, *Colloid Interface Sci. Commun.* 35 (2020), 100247, <https://doi.org/10.1016/j.colcom.2020.100247>.
- [90] T. Umair Wani, A. Hamid Rather, R. Saleem Khan, J. Macossay, A.H. Jadhav, P. M. Srinivasappa, A. Abdal-hay, S. Rather, F.A. Sheikh, Titanium dioxide functionalized multi-walled carbon nanotubes, and silver nanoparticles reinforced polyurethane nanofibers as a novel scaffold for tissue engineering applications, *J. Ind. Eng. Chem.* 121 (2023) 200–214, <https://doi.org/10.1016/j.jiec.2023.01.024>.
- [91] B. Şimşek, T. Uygunoğlu, Ö.F. Dilmaç, Comparative evaluation of the effectiveness of PTFE nanoparticles on cement pastes properties with multi-wall carbon nanotubes, graphene oxide and silver nanoparticles, *Constr. Build. Mater.* 319 (2022), 126077, <https://doi.org/10.1016/j.conbuildmat.2021.126077>.
- [92] L. Hu, Z. Kang, Enhanced flexible polypropylene fabric with silver/magnetic carbon nanotubes coatings for electromagnetic interference shielding, *Appl. Surf. Sci.* 568 (2021), 150845, <https://doi.org/10.1016/j.apsusc.2021.150845>.
- [93] F. Taherkhani, Hydrogen storage via silver–aluminum bimetallic nanoparticle supported on different shapes defect on carbon nanotube, *Int. J. Hydrog. Energy* 47 (2022) 5380–5392, <https://doi.org/10.1016/j.ijhydene.2021.11.142>.
- [94] D. Park, M. Kim, J. Kim, Preparation and structure dependent thermoelectric properties of flexible N-type nanostructured silver(I) selenide/multi-walled carbon nanotube composite film, *Appl. Surf. Sci.* 613 (2023), 156150, <https://doi.org/10.1016/j.apsusc.2022.156150>.
- [95] O.K. Abudayyeh, A. Chavez, S.M. Han, B. Rounsaville, V. Upadhyaya, A. Rohatgi, Silver-carbon-nanotube composite metallization for increased durability of silicon solar cells against cell cracks, *Sol. Energy Mater. Sol. Cells* 225 (2021), 111017, <https://doi.org/10.1016/j.solmat.2021.111017>.
- [96] N.M. Deghiedy, N.M. Yousif, H.M. Hosni, M.R. Balboul, Silver-modified electrodes based on amorphous MnO₂/ carbon nanotube: Multicomponent approach to enhance the performance of supercapacitors, *J. Phys. Chem. Solids* 161 (2022), 110445, <https://doi.org/10.1016/j.jpcs.2021.110445>.
- [97] X. Huang, D. Wang, L. Hu, J. Song, Y. Chen, Preparation of a novel antibacterial coating precursor and its antibacterial mechanism, *Appl. Surf. Sci.* 465 (2019) 478–485, <https://doi.org/10.1016/j.apsusc.2018.09.160>.
- [98] S.K. Yadav, H.E. Atyia, S.S. Fouad, A. Sharma, N. Mehta, Study of linear and non-linear optoelectronic properties of thermally grown thin films of amorphous selenium doped with graphene, multiwalled carbon nanotubes, and silver nanoparticles, *Diam. Relat. Mater.* 136 (2023), 110030, <https://doi.org/10.1016/j.diamond.2023.110030>.
- [99] W. Lv, J. Hu, J. Liu, C. Xiong, F. Zhu, Porosity effect on the mechanical properties of nano-silver solder, *Nanotechnol* 34 (2023), 165701, <https://doi.org/10.1088/1361-6528/ACB4F3>.
- [100] R.K. Goyal, A.N. Tiwari, Y.S. Negi, Microhardness of PEEK/ceramic micro- and nanocomposites: correlation with Halpin–Tsai model, *Mater. Sci. Eng. A* 491 (2008) 230–236, <https://doi.org/10.1016/j.msea.2008.01.091>.
- [101] A.O. Adegbenjo, B.A. Obadele, P.A. Olubambi, Densification, hardness and tribological characteristics of MWCNTs reinforced Ti6Al4V compacts

- consolidated by spark plasma sintering, *J. Alloy. Compd.* 749 (2018) 818–833, <https://doi.org/10.1016/j.jallcom.2018.03.373>.
- [102] J.D. Kim, H. Yun, G.C. Kim, C.W. Lee, H.C. Choi, Antibacterial activity and reusability of CNT-Ag and GO-Ag nanocomposites, *Appl. Surf. Sci.* 283 (2013) 227–233, <https://doi.org/10.1016/j.apsusc.2013.06.086>.
- [103] M.A.L. Dos Reis, N.M. Barbosa Neto, M.E.S. De Sousa, P.T. Araujo, S. Simões, M. F. Vieira, F. Viana, C.R.L. Loayza, D.J.A. Borges, D.C.S. Cardoso, P.D.C. Assunção, E.M. Braga, Raman spectroscopy fingerprint of stainless steel-MWCNTs nanocomposite processed by ball-milling, *AIP Adv.* 8 (2018), 015323, <https://doi.org/10.1063/1.5018745>.
- [104] M.E. David, R.-M. Ion, R.M. Grigorescu, L. Iancu, A.M. Holban, A.I. Nicoara, E. Alexandrescu, R. Somoghi, M. Ganciarov, G. Vasilevici, A.I. Gheboianu, Hybrid materials based on multi-walled carbon nanotubes and nanoparticles with antimicrobial properties, *Nanomater* 11 (2021) 1415, <https://doi.org/10.3390/nano11061415>.
- [105] S.-G. Kim, O.-K. Park, J.H. Lee, B.-C. Ku, Layer-by-layer assembled graphene oxide films and barrier properties of thermally reduced graphene oxide membranes, *Carbon Lett.* 14 (2013) 247–250, <https://doi.org/10.5714/cl.2013.14.4.247>.
- [106] A.T.S.C. Brandão, S. Rosoiu, R. Costa, O.A. Lazar, A.F. Silva, L. Anicai, C. M. Pereira, M. Enachescu, Characterization and electrochemical studies of MWCNTs decorated with Ag nanoparticles through pulse reversed current electrodeposition using a deep eutectic solvent for energy storage applications, *J. Mater. Res. Technol.* 15 (2021) 342–359, <https://doi.org/10.1016/j.jmrt.2021.08.031>.
- [107] J. Dias Corpa Tardelli, A.C. Duarte Firmino, I. Ferreira, A. Cândido dos Reis, Influence of the roughness of dental implants obtained by additive manufacturing on osteoblastic adhesion and proliferation: a systematic review, *Heliyon* 8 (2022), e12505, <https://doi.org/10.1016/j.heliyon.2022.e12505>.
- [108] B. Ren, Y. Wan, C. Liu, H. Wang, M. Yu, X. Zhang, Y. Huang, Improved osseointegration of 3D printed Ti-6Al-4V implant with a hierarchical micro/nano surface topography: an in vitro and in vivo study, *Mater. Sci. Eng. C.* 118 (2021), 111505, <https://doi.org/10.1016/j.msec.2020.111505>.
- [109] N. Walter, T. Stich, D. Docheva, V. Alt, M. Rupp, Evolution of implants and advancements for osseointegration: a narrative review, *Inj* 53 (2022) S69–S73, <https://doi.org/10.1016/j.injury.2022.05.057>.
- [110] C.A. Isaza M, B. Zuluaga D, J.S. Rudas, H.A. Estupiñán D, J.M. Herrera R, J. M. Meza, Mechanical and Corrosion Behavior of Plasma Electrolytic Oxidation Coatings on AZ31B Mg Alloy Reinforced with Multiwalled Carbon Nanotubes, *J. Mater. Eng. Perform.* 29 (2020) 1135–1145, <https://doi.org/10.1007/s11665-020-04633-z>.
- [111] M.L. Masheane, L.N. Nthunya, S.P. Malinga, E.N. Nxumalo, B.B. Mamba, S. D. Mhlanga, Synthesis of Fe-Ag/f-MWCNT/PES nanostructured-hybrid membranes for removal of Cr(VI) from water, *Sep. Purif. Technol.* 184 (2017) 79–87, <https://doi.org/10.1016/j.seppur.2017.04.018>.
- [112] L. Macevele, K. Moganedi, T. Magadzu, Investigation of antibacterial and fouling resistance of silver and multi-walled Carbon Nanotubes Doped Poly(Vinylidene Fluoride-co-Hexafluoropropylene) Composite Membrane, *Membr. (Basel)* 7 (2017) 35, <https://doi.org/10.3390/membranes7030035>.
- [113] E. Dlugon, W. Simka, A. Fraczek-Szczypta, W. Niemiec, J. Markowski, M. Szymanska, M. Blazewicz, Carbon nanotube-based coatings on titanium, *Bull. Mater. Sci.* 38 (2015) 1339–1344, <https://doi.org/10.1007/s12034-015-1019-4>.
- [114] S. Singh, C. Srivastava, Effect of carbon nanotube incorporation on the evolution of morphology, phase and compositional homogeneity, surface oxide chemistry and corrosion behaviour of electrodeposited FeCuMnNiCo-carbon nanotube composite coatings, *Electrochim. Acta* 439 (2023), 141639, <https://doi.org/10.1016/j.electacta.2022.141639>.
- [115] C. García-Cabezón, V. Godinho, C. Pérez-González, Y. Torres, F. Martín-Pedrosa, Electropolymerized polypyrrole silver nanocomposite coatings on porous Ti substrates with enhanced corrosion and antibacterial behavior for biomedical applications, *Mater. Today Chem.* 29 (2023), <https://doi.org/10.1016/j.mtchem.2023.101433>.
- [116] B. Wang, Y. Li, S. Wang, F. Jia, A. Bian, K. Wang, L. Xie, K. Yan, H. Qiao, H. Lin, J. Lan, Y. Huang, Electrodeposited dopamine/strontium-doped hydroxyapatite composite coating on pure zinc for anti-corrosion, antimicrobial and osteogenesis, *Mater. Sci. Eng. C.* 129 (2021), 112387, <https://doi.org/10.1016/j.msec.2021.112387>.